

ONLINE FIRST

Default Mode Network Disruption Secondary to a Lesion in the Anterior Thalamus

David T. Jones, MD; Farrah J. Mateen, MD; Claudia F. Lucchinetti, MD; Clifford R. Jack Jr, MD; Kirk M. Welker, MD

Objective: To describe the neuroanatomical correlations of an isolated lesion in the anterior thalamus using functional imaging in a 40-year-old man with multiple sclerosis.

Design: Case report with 10 cognitively normal controls.

Setting: Mayo Clinic, Rochester, Minnesota.

Patient: A 40-year-old man with a 2-week course of acute-onset amnesia, abulia, poor concentration, hyper-somnolence, and reclusiveness.

Intervention: Functional magnetic resonance imaging.

Results: Magnetic resonance imaging demonstrated a large gadolinium-enhancing plaque in the left anterior thalamus and other demyelinating plaques in the sub-

cortical and periventricular white matter, consistent with the diagnosis of multiple sclerosis. His symptoms persisted at the 7-month follow-up. The patient's resting state functional magnetic resonance image demonstrated an asymmetric disruption of the posterior cingulate portion of the default mode network ipsilateral to the left thalamic lesion.

Conclusions: A large multiple sclerosis plaque in the deep gray matter altered the resting state functional connectivity in a patient presenting with pure cognitive dysfunction. Such altered connectivity may underlie cognitive symptoms in neurologic disease. In addition, this case provides lesional evidence of default mode network circuitry involving the pathways of the circuit of Papez.

Arch Neurol. 2011;68(2):242-247. Published online October 11, 2010. doi:10.1001/archneurol.2010.259

IN 1937, PAPEZ¹ DESCRIBED A CLASSICAL circuit important in human memory and emotion. Anatomically, this circuit includes projections from the subicular complex to the mamillary nuclei that project to the anterior nucleus of the thalamus. The anterior nucleus of the thalamus, in turn, projects to the posterior cingulate cortex back to the hippocampal formation. If this loop is disrupted, severe amnesia may result.

Functional magnetic resonance imaging (fMRI) analysis techniques using low-frequency fluctuations (0.08-0.01 HZ) in the blood oxygen level-dependent (BOLD) T2* signal have consistently identified global brain networks that are anatomically and functionally related.²⁻⁴ Most of these investigations have examined BOLD signal fluctuations in the resting brain, and the subsequently identified networks have been termed *resting state networks* (RSN). The relationship of RSN to cognitive function is uncertain; if they are related to normal cognitive function, then it would be

reasonable to hypothesize that an acute change in cognitive function would lead to a measurable change in a particular RSN or its relationship to other RSNs.

We attempt to validate this line of reasoning using an illustrative case study of acute cognitive dysfunction associated with a lesion in the anatomical circuit of Papez, analyzed using a resting-state fMRI method known as independent component analysis (ICA). Independent component analysis is a model-free, data-driven fMRI analysis technique that can be used to define the spatial and temporal relationship of low-frequency BOLD fluctuations across the resting brain to identify RSN.⁵ In addition, we conducted a connectivity analysis using correlations of the BOLD time course derived from a seed approximating the patient's lesion in the anterior thalamus.

The default mode network (DMN) is an RSN composed of multiple brain regions that are more active during passive rest than during attention-demanding tasks.⁶ The DMN is composed of the pos-

Author Affiliations:
Departments of Neurology (Drs Jones, Mateen, and Lucchinetti) and Radiology (Drs Jack and Welker), Mayo Clinic, Rochester, Minnesota.

terior cingulate cortex (PCC), medial prefrontal cortex, inferior parietal lobule, lateral temporal cortex, and hippocampal formation.⁷ The functional circuits that underlie the coordination of these diverse brain structures are currently unknown. However, these structures are within limbic, paralimbic, or heteromodal association cortices, and we hypothesize that they are interconnected via anterior and posterior limbic circuitry. The posterior limbic circuitry has commonly been referred to as the circuit of Papez,¹ and its disruption has been implicated in the cognitive dysfunction present in conditions such as Wernicke-Korsakoff syndrome,⁸ focal hemorrhage,⁹ and mesial temporal sclerosis.¹⁰ In this article we use resting-state fMRI to compare the DMN activity of 10 healthy control subjects with that of a 40-year-old man with an acute lesion in the circuit of Papez leading to cognitive dysfunction.

REPORT OF A CASE

A 40-year-old, right-handed man experienced acute onset of personality change, hypersomnolence, and cognitive decline marked by poor concentration. He began sleeping more than 12 hours per day. He forgot how to operate machinery at work and became carefree and mellow.

Ten years earlier, he had an isolated 2-week episode of foot numbness. He smoked cigarettes daily but otherwise had no relevant medical history and took no medications.

At the time of referral, cognitive symptoms had been present for 2 weeks. He scored 22 of a 38 possible points on the short test of mental status,¹¹ losing points for orientation (score, 3 of a possible 8), calculation (2 of 4), abstraction (0 of 3), attention (5 of 7), learning (3 of 4), information (3 of 4), and recall (2 of 4). He had global cognitive dysfunction, and language was impaired. He was especially poor at naming (correctly identifying 2 of 4 objects), describing a picture, and writing. He had diffuse mild hyperreflexia on examination of deep tendon reflexes and bilateral plantar extensor responses to Chaddock maneuver. Findings of neurological examination were otherwise normal.

Electroencephalogram showed mild slowing over the left temporal region without epileptiform discharges. Cerebral spinal fluid analysis demonstrated oligoclonal banding and an elevated IgG synthesis rate. Magnetic resonance imaging revealed scattered T2 hyperintense white matter lesions consistent with demyelinating plaques, with the single largest lesion involving the left anterior thalamus (**Figure 1**). The anterior thalamic lesion was the only gadolinium-enhancing plaque. He received 1 g of methylprednisolone intravenously daily for 5 days with some improvement in motivation and language by day 3; however, he scored lower (19 points) on mental status retesting 1 month later. This improved to 30 points at 5 months with persistent short-term memory loss. Executive dysfunction and inappropriate laughter were noted. At the 7-month follow up, he remained less engaged in his daily activities and reclusive but was able to return to work full-

time. He received beta interferon and, later, natalizumab for long-term management.

METHODS

Resting-state gradient, echo-planer BOLD fMRI sequences were obtained for the patient 12 days after initial presentation while he was still symptomatic using a General Electric 3T Signa HDx (Waukesha, Wisconsin) scanner at 14.0 level software (8-channel head coil; 30 axial slices; thickness, 5 mm without gap; time to repetition, 2000 milliseconds; echo time, 30 milliseconds; flip angle, 90°; in-plane resolution, 64 × 64; field of view, 220 × 220 mm; 200 volumes), and a spoiled gradient recalled T1-weighted structural image was obtained for coregistration of functional data. Ten cognitively normal volunteers (mean [SD] age, 44.2 [9.16] years; 3 male) were evaluated with the same imaging protocol for comparison. All participants were instructed to rest comfortably in the scanner with their eyes open. The images were preprocessed using statistical parametric mapping (SPM) software (Wellcome Department of Cognitive Neurology, University College London, London, England), with the SPM5 version implemented in MATLAB (Mathworks Inc, Sherborn, Massachusetts). Preprocessing steps included discarding the first 10 volumes to allow for scanner and cognitive equilibrium, rigid body motion correction, slice timing correction, normalization to Montreal Neurologic Institute standard space, coregistration to spoiled gradient recalled T1-weighted structural image, and smoothing with an 8-mm full width at half maximum Gaussian filter. These images were then analyzed using Group ICA of fMRI Toolbox software with individual subject maps produced with the dual-regression method.¹² The independent components were visually inspected to identify the DMN based on its typical appearance. The DMN for the subject was then overlaid on the coregistered structural MRI, and the group DMN was overlaid on a representative control subject's coregistered structural MRI. To assess variability in the individual DMN components produced, the average *z* score from each subject's component were extracted from right and left seed regions using the MarsBar toolbox (<http://marsbar.sourceforge.net/>). The seed regions of interest were defined using the precuneus and PCC regions from the automated anatomical labeling atlas.¹³ To quantitatively compare the patient's DMN with the control group's, the 2-sample *t* test function in SPM5 was used in a method similar to the commonly used clinical comparison of individual subjects' positron emission tomographic scans to control groups.¹⁴ Results are reported as significant if they exceed a voxel-level false discovery rate corrected $P < .01$ with a corrected cluster level $P < .001$. A similar statistical comparison was performed for multiple other easily identifiable RSN in this data set (ie, right central executive, left central executive, visual, auditory, and sensory-motor networks).

To further investigate the relationship of the thalamus to RSNs, a seed-based connectivity analysis was performed using the resting-state fMRI data analysis toolkit (<http://www.restfmri.net>), SPM5, and in-house developed software implemented in MATLAB. Prior to performing seed analysis, the resting-state images were put through several additional standard preprocessing steps that included linear detrending to correct for signal drift, 0.01- to 0.08-Hz bandpass filtering to reduce non-neuronal contributions to BOLD fluctuations, and regression correction for spurious variables such as rigid body transformation motion effects, global mean signal, and white matter and cerebral spinal fluid signal.¹⁵ Then, a 5-mm radius seed region of interest (Montreal Neurological Institute coordinates, -8, -9, -1) approximating the position of the subject's thalamic lesion was used to extract the BOLD time course for each

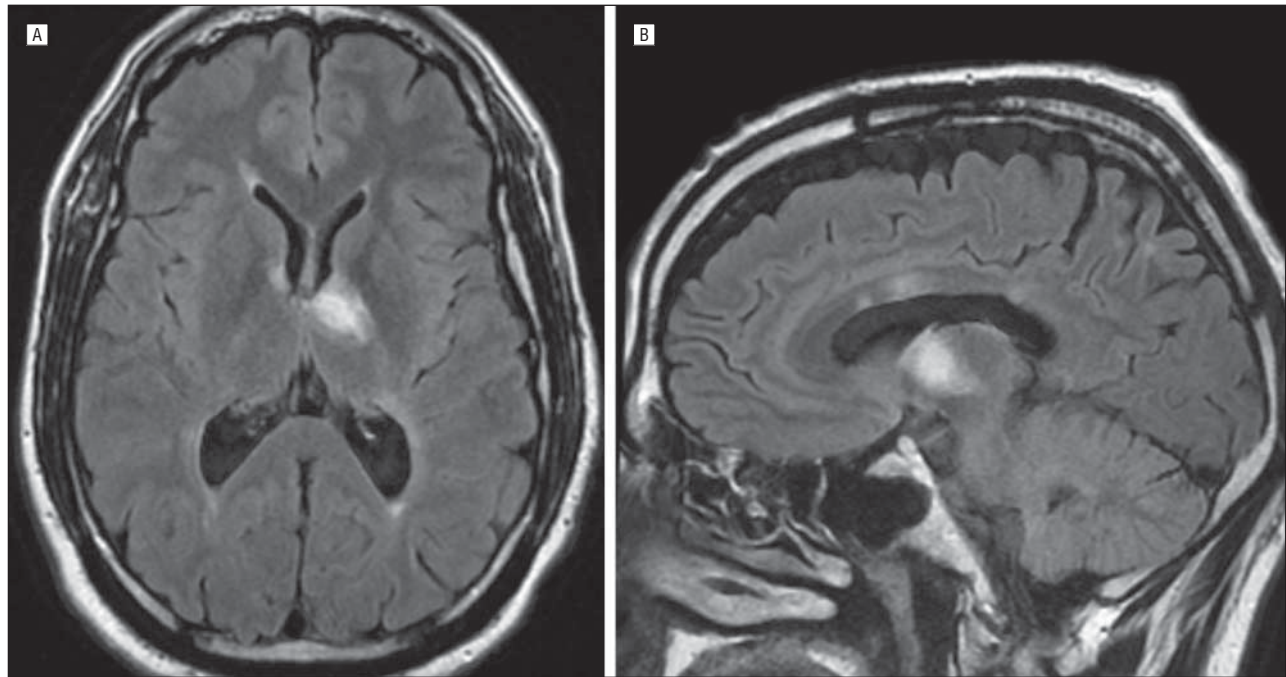


Figure 1. Structural magnetic resonance imaging of the brain demonstrating the symptomatic lesion in the left anterior thalamus, which is T2-hyperintense on axial (A) and sagittal (B) fluid-attenuated inversion recovery sequences.

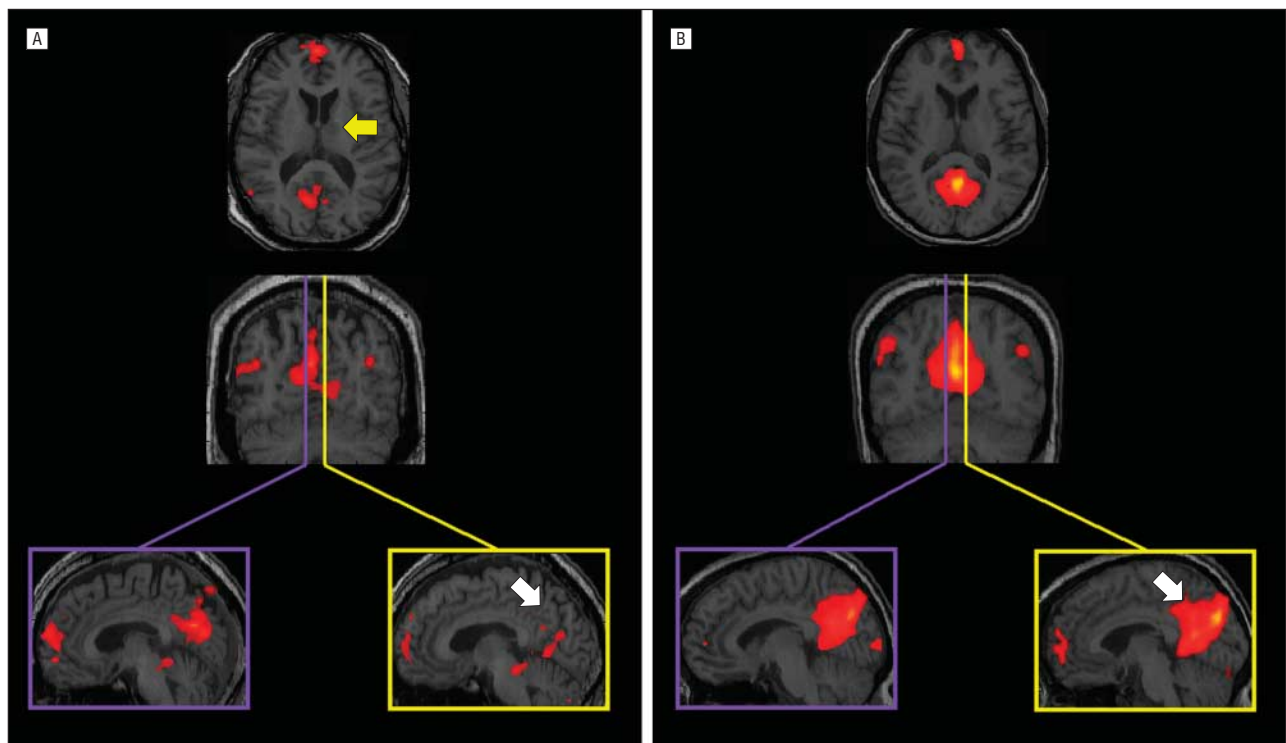


Figure 2. Resting-state functional magnetic resonance imaging analyzed with independent component analysis demonstrates the default mode network (DMN). The patient's DMN overlaid on a coregistered structural magnetic resonance image (A) demonstrates an asymmetric disruption of the posterior cingulate (white arrow) portion of the network ipsilateral to the left thalamic lesion (yellow arrow). The control group's (n=10) DMN overlaid on a representative control subject's coregistered structural magnetic resonance image (B) demonstrates the full symmetric extent of the posterior cingulate (arrow) cortex's contribution to the network in cognitively normal controls.

participant. The low-frequency time course for each participant was then correlated with every other voxel in the brain using the Pearson correlation coefficient. Regions with a fluctuating time course in phase with the region of interest time course have positive correlation values, and regions with out-

of-phase fluctuations have negative correlation values. To evaluate if regions displayed a 90° out-of-phase lagging relationship (which would have a correlation value near 0), a lagged correlation analysis was performed by shifting the region of interest reference time course for each subject by a lag correspond-

ing to 90° of the reference time-course period and repeating the correlation analysis. This lagged correlation approach may have the potential to elucidate a temporal lag in a functional relationship along a circuit.¹⁶ After performing a Fischer *r*-to-*z* transformation for all images, the subject's lagged voxel-wise connectivity map was compared with those of controls (given that the lagged correlational map was consistent with 2 key DMN regions). A similar SPM statistical procedure used for the ICA analysis was used for the lagged correlation comparison. Results were reported as significant if they exceed a voxel-level false discover rate corrected $P < .01$ with a corrected cluster level $P < .001$.

RESULTS

The patient's ICA-identified DMN demonstrated an asymmetric disruption of the PCC portion of the default mode network ipsilateral to the left thalamic lesion (**Figure 2, A**). The group ICA of the resting state MRI produced the typical symmetric spatial extent of the DMN (Figure 2,

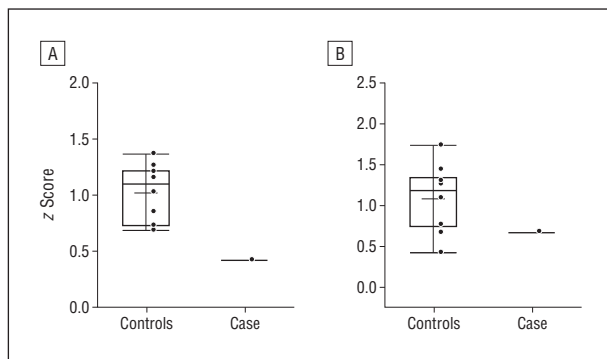


Figure 3. Variability in precuneus/posterior cingulate cortex contributions to the default mode network. The average *z* score within the precuneus/posterior cingulate cortex regions of the independent component analysis-identified default mode networks are displayed in a box plot for the controls and the index case for the left (A) and right (B) hemispheres.

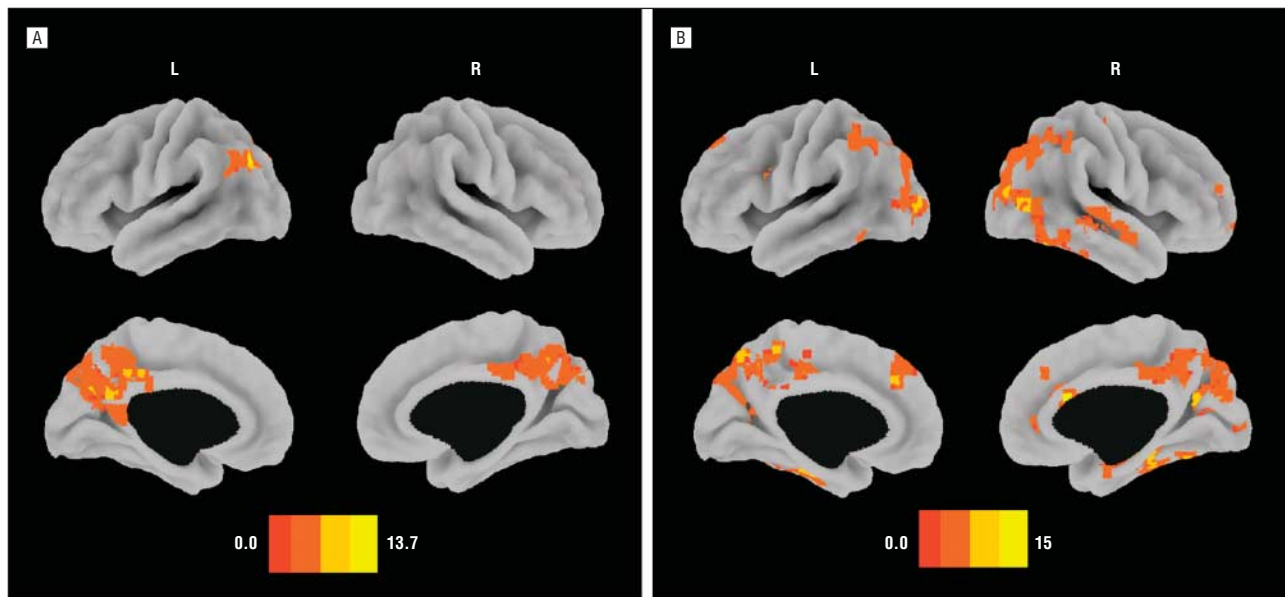


Figure 4. Subject vs group comparison of connectivity. The statistical comparison of the patient's default mode network (DMN) connectivity vs the control group's connectivity is displayed on surface projections using Caret software (<http://www.nitrc.org/projects/caret/>) for the independent component analysis-identified DMN (A) and the lagged-correlation identified DMN (B). Both analysis techniques of the DMN revealed a reduction in the patient's connectivity compared with that of controls in the precuneus and posterior cingulate cortex. The color bar below each figure encodes the *t* value for statistically significant regions of decreased connectivity. Both surface projections are displayed at a statistical threshold of a voxel-level false discover rate $P < .05$ and corrected cluster $P < .001$. L indicates left; R, right.

B). None of the control subjects' individual DMNs displayed right to left asymmetry. The right and left PCC/precuneus contribution to every participant's DMN identified using ICA is displayed in a box plot (**Figure 3**). Statistical analysis of the patient's ICA-identified DMN compared with that of the control group demonstrated a reduction in the patient's DMN connectivity in the PCC, precuneus, and left inferior parietal lobe (**Figure 4, A**). No statistically significant difference was found in any other RSN examined.

The anterior thalamus seed-based connectivity analysis demonstrated significant group correlations (**Figure 5**) and patient to group comparison (Figure 4 and Figure 5). The group in-phase relationship mainly consisted of bilateral thalamic regions and regions of the saliency network (ie, bilateral fronto-insular cortices and anterior cingulate), with some additional in-phase relationship with the PCC. After time-lagged correlation, the relationship no longer revealed any thalamic contribution (as expected) but did reveal a relationship with 2 key DMN nodes (the precuneus and medial prefrontal cortex). The out-of-phase relationship consisted primarily of sensorimotor regions and the orbitofrontal cortex.

The statistical analysis of the patient's time-lagged correlational relationship compared with that of the group revealed a similar decrease in DMN regions, as was observed for the ICA analysis, which included the PCC and precuneus (Figure 4 and Figure 5).

COMMENT

The index case and resting state fMRI analysis illustrate 2 key points. First, deep gray matter lesions may contribute to cognitive dysfunction in neurologic illness. Second, anterior thalamic lesions along the circuit of Pa-

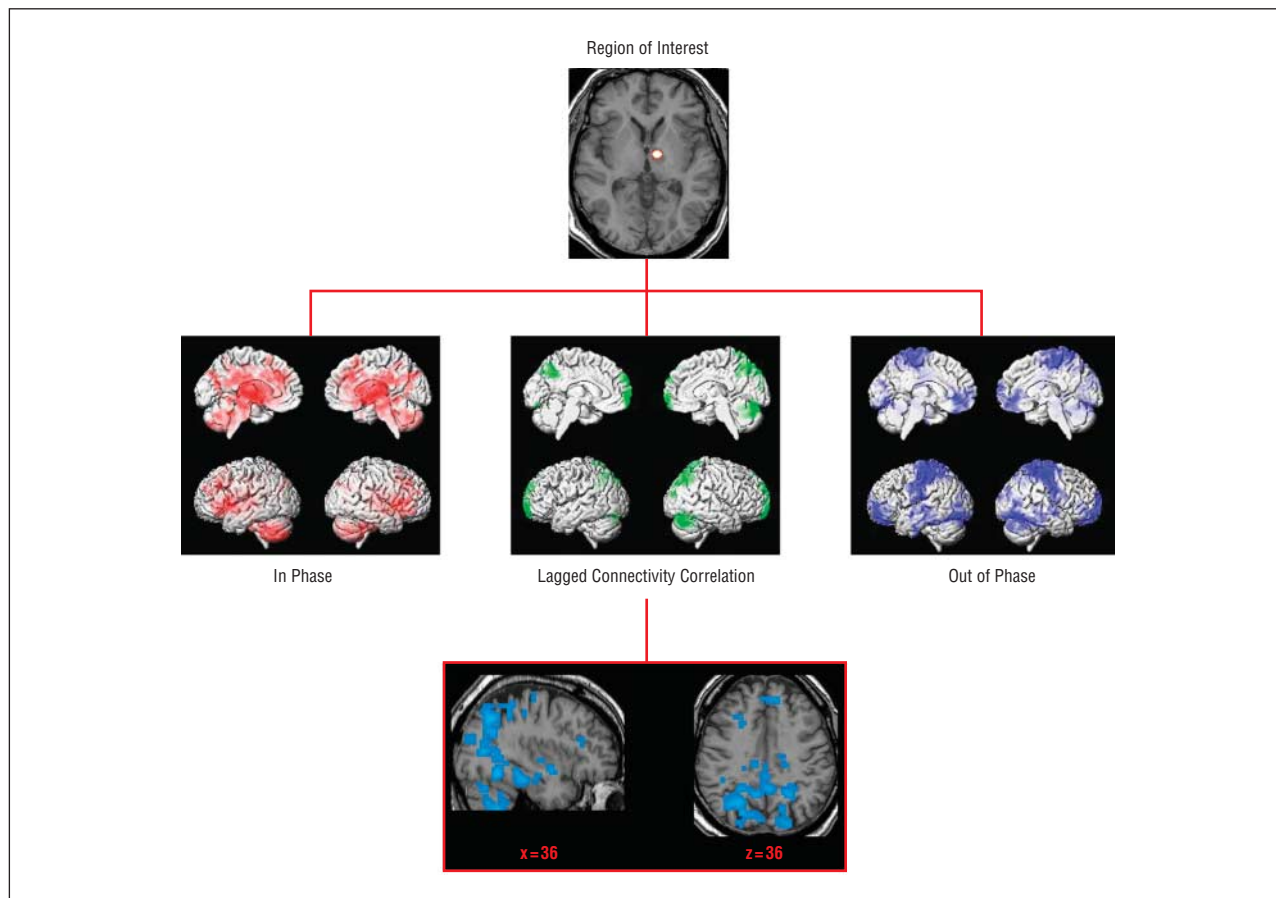


Figure 5. Anterior thalamus seed-based time-course analysis. A region of interest approximating the patient's lesion is displayed over an axial slice of the patient's structural magnetic resonance imaging. The blood oxygen level–dependent time course for every participant was then extracted from this region of interest and correlated with every other voxel in the brain. Regions with positive correlation values are assumed to have an in-phase connectivity relationship, while regions with negative correlation values are assumed to have an out-of-phase connectivity relationship. Regions that displayed correlation values near 0 with the reference region of interest time course but displayed positive correlation values with the lagged time course represent the lagged connectivity relationship. The statistical comparison of the patient's lagged-correlation voxelwise connectivity to the control group is displayed on a sagittal and axial slice of the subject's structural image with corresponding Montreal Neurological Institute coordinates below each slice (see also Figure 4). Displayed using MRlcro (<http://www.cabiatl.com/mricro/>) at a statistical threshold of a voxel-level false discover rate $P < .05$ and corrected cluster $P < .001$.

pez disrupt the DMN. The DMN is the brain state that dominates in a resting non-task-directed mode of brain function.¹⁷ To perform task-directed activities, the activity of the DMN subsides as task-relevant regions of the brain predominate. Another RSN known as the saliency network has been theorized to facilitate the switching of brain states from the DMN to task-relevant networks.¹⁸ The patient that we describe presented with a lesion in the thalamus that disrupted the DMN and potentially impaired his ability to switch from a default mode of brain function to a task-related state of brain function. This manifested clinically as acute cognitive dysfunction in multiple domains and persistent short-term memory impairment. Therefore, disruption of anatomical connections also manifest in altered RSN functional connectivity.

This case study supports the conclusion that RSN are related to cognitive function and have the potential to advance the understanding of cognitive dysfunction in clinical settings. In addition, this case provides lesional evidence of DMN circuitry involving the pathways of the circuit of Papez. A previous positron emission tomography study has demonstrated a similar impairment in PCC function with circuit of Papez lesions secondary to alcoholic Korsakoff syn-

drome.¹⁹ However, resting-state fMRI DMN analysis provides a novel noninvasive means of investigating the relationship between anatomic lesions and cognitive symptoms.

Accepted for Publication: August 17, 2010.

Published Online: October 11, 2010. doi:10.1001/archneurol.2010.259

Correspondence: David T. Jones, MD, Department of Neurology, Mayo Clinic, 200 First St SW, Rochester, MN 55905 (jones.david@mayo.edu).

Author Contributions: Dr Jones had full access to all of the data in the study and takes responsibility for the integrity of the data and the accuracy of the data analysis. *Study concept and design:* Jones, Mateen, and Welker. *Acquisition of data:* Jones, Mateen, Lucchinetti, and Welker. *Analysis and interpretation of data:* Jones, Mateen, and Jack. *Drafting of the manuscript:* Jones and Mateen. *Critical revision of the manuscript for important intellectual content:* Jones, Mateen, Lucchinetti, Jack, and Welker. *Statistical analysis:* Jones. *Administrative, technical, and material support:* Jones, Mateen, Jack, and Welker. *Study supervision:* Lucchinetti and Welker.

Financial Disclosure: None reported.

REFERENCES

1. Papez JW. A proposed mechanism of emotion. *Arch Neurol Psychiatry*. 1937;38:725-743.
2. Auer DP. Spontaneous low-frequency blood oxygenation level-dependent fluctuations and functional connectivity analysis of the "resting" brain. *Magn Reson Imaging*. 2008;26(7):1055-1064.
3. Damoiseaux JS, Rombouts SA, Barkhof F, et al. Consistent resting-state networks across healthy subjects. *Proc Natl Acad Sci U S A*. 2006;103(37):13848-13853.
4. van den Heuvel MP, Mandl RC, Kahn RS, Hulshoff Pol HE. Functionally linked resting-state networks reflect the underlying structural connectivity architecture of the human brain. *Hum Brain Mapp*. 2009;30(10):3127-3141.
5. Beckmann CF, DeLuca M, Devlin JT, Smith SM. Investigations into resting-state connectivity using independent component analysis. *Philos Trans R Soc Lond B Biol Sci*. 2005;360(1457):1001-1013.
6. Greicius MD, Krasnow B, Reiss AL, Menon V. Functional connectivity in the resting brain: a network analysis of the default mode hypothesis. *Proc Natl Acad Sci U S A*. 2003;100(1):253-258.
7. Buckner RL, Andrews-Hanna JR, Schacter DL. The brain's default network: anatomy, function, and relevance to disease. *Ann N Y Acad Sci*. 2008;1124:1-38.
8. Sullivan EV, Pfefferbaum A. Neuroimaging of the Wernicke-Korsakoff syndrome. *Alcohol Alcohol*. 2009;44(2):155-165.
9. Oikawa H, Sasaki M, Tamakawa Y, Kamei A. The circuit of Papez in mesial temporal sclerosis: MRI. *Neuroradiology*. 2001;43(3):205-210.
10. Valenstein E, Bowers D, Verfaellie M, Heilman KM, Day A, Watson RT. Retro-splenic amnesia. *Brain*. 1987;110(pt 6):1631-1646.
11. Kokmen E, Smith GE, Petersen RC, Tangalos E, Ivnik RC. The short test of mental status: correlations with standardized psychometric testing. *Arch Neurol*. 1991;48(7):725-728.
12. Calhoun VD, Adali T, Pearson GD, Pekar JJ. A method for making group inferences from functional MRI data using independent component analysis. *Hum Brain Mapp*. 2001;14(3):140-151.
13. Tzourio-Mazoyer N, Landeau B, Papathanassiou D, et al. Automated anatomical labeling of activations in SPM using a macroscopic anatomical parcellation of the MNI MRI single-subject brain. *Neuroimage*. 2002;15(1):273-289.
14. Signorini M, Paulesu E, Friston K, et al. Rapid assessment of regional cerebral metabolic abnormalities in single subjects with quantitative and nonquantitative [18F]FDG PET: a clinical validation of statistical parametric mapping. *Neuroimage*. 1999;9(1):63-80.
15. Fox MD, Snyder AZ, Vincent JL, Corbetta M, Van Essen DC, Raichle ME. The human brain is intrinsically organized into dynamic, anticorrelated functional networks. *Proc Natl Acad Sci U S A*. 2005;102(27):9673-9678.
16. Chang C, Glover GH. Time-frequency dynamics of resting-state brain connectivity measured with fMRI. *Neuroimage*. 2010;50(1):81-98.
17. Raichle ME, MacLeod AM, Snyder AZ, Powers WJ, Gusnard DA, Shulman GL. A default mode of brain function. *Proc Natl Acad Sci U S A*. 2001;98(2):676-682.
18. Sridharan D, Levitin DJ, Menon V. A critical role for the right fronto-insular cortex in switching between central-executive and default-mode networks. *Proc Natl Acad Sci U S A*. 2008;105(34):12569-12574.
19. Joyce EM, Rio DE, Ruttimann UE, et al. Decreased cingulate and precuneate glucose utilization in alcoholic Korsakoff's syndrome. *Psychiatry Res*. 1994;54(3):225-239.

Announcement

Visit www.archneurolog.com. As an individual subscriber, you may elect to be contacted when a specific article is cited. Receive an e-mail alert when the article you are viewing is cited by any of the journals hosted by HighWire. You will be asked to enter the volume, issue, and page number of the article you wish to track. Your e-mail address will be shared with other journals in this feature; other journals' privacy policies may differ from *JAMA & Archives Journals*. You may also sign up to receive an e-mail alert when articles on particular topics are published.